Geophysical Journal International

Geophys. J. Int. (2013) **195,** 1132–1140
Advance Access publication 2013 August 8

doi: 10.1093/gji/ggt276

Timing of a large volcanic flank movement at Piton de la Fournaise Volcano using noise-based seismic monitoring and ground deformation measurements

D. Clarke,[1] F. Brenguier,[2] J.-L. Froger,[3] N. M. Shapiro,[1] A. Peltier[1] and T. Staudacher[4]

[1]*Institut de Physique du Globe de Paris, Sorbonne Paris Cité, CNRS, France. E-mail: danielclarke1@gmail.com*
[2]*Institut des Sciences de la Terre, Université Joseph Fourier, Grenoble, France*
[3]*Laboratoire Magmas et Volcans, Observatoire de Physique du Globe de Clermont-Ferrand, France*
[4]*Observatoire Volcanologique du Piton de la Fournaise, IPGP, Sorbonne Paris Cité, CNRS, France*

Accepted 2013 July 9. Received 2013 June 19; in original form 2013 January 24

SUMMARY

In volcanic domains, magma transport and pressure build-up induce high stress–strain perturbations in the surrounding volcanic edifice that may lead to volcanic flank movements and possible instability. In this study, we focus on the 2007 March–April episode of volcanic activity at Piton de la Fournaise (PdF) Volcano, La Réunion Island. This episode was associated with a large volume of emitted lava (240×10^6 m^3) and a 340-m caldera collapse. We present observations of continuous seismic velocity changes measured using cross-correlations of ambient seismic noise over 10 yr at PdF. Overall, we observe a large velocity reduction starting a few days prior to the major 2007 April 2 eruption. Comparison of seismic velocity change measurements with observations of deformation from InSAR and GPS shows that the seismic velocity reduction coincided with a widespread flank movement starting at the time of injection of magma to feed an initial eruption, a few days before the 2007 April 2 eruption. We emphasize the potential of noise-based seismic velocity change measurements, together with geodetic observations, to detect and monitor possibly hazardous slope instabilities.

Key words: Interferometry; Satellite geodesy; Radar interferometry; Volcano seismology; Volcano monitoring; Indian Ocean.

1 INTRODUCTION

Among the risks associated with volcanic activity, the destabilization of volcanic edifices can have catastrophic consequences for nearby populations. These are not only the direct effects of the large volume of material that is mobilized in such events (Devoli *et al.* 2009), but also indirect effects such as the eruption of depressurized magma chambers (Alidibirov & Dingwell 1996) and, in the case of coastal and oceanic volcanoes, tsunami generation (Ward & Day 2003). After the dramatic collapse of the northern flank of Mount St Helens in 1980 May (Lipman & Mullineaux 1981) and the discovery of large debris avalanche deposits in the Hawaii island chain (Moore *et al.* 1989), increased attention has been paid to edifice collapse events and the hazard they represent (McGuire 1996). Globally, these are estimated to have occurred on average four times during each of the last five centuries (Siebert 1992) and their deposits have been identified around volcanoes such as Mauna Loa (Lipman *et al.* 1988), Mt Etna (Calvari *et al.* 1998; Pareschi *et al.* 2006), Tenerife (Watts & Masson 1995), Socompa (Francis *et al.* 1985), Mombacho (De Vries & Francis 1997) and La Réunion Island (Labazuy 1996; Le Friant *et al.* 2011). Such volcanic flank movements and possible destabilizations have been recognized as being possibly triggered by magma injections (Walter *et al.* 2005; Famin & Michon 2010).

Recently, the analysis of ambient seismic noise has developed into a promising tool for monitoring the deformation within the Earth's crust at depth. For example, ambient seismic noise cross-correlations have been exploited to monitor both volcanic interiors (Sens-Schönfelder & Wegler 2006; Brenguier *et al.* 2008b; Mordret *et al.* 2010) and active fault zones (Wegler & Sens-Schönfelder 2007; Brenguier *et al.* 2008a). These works rely on both theoretical and applied results, which show that the Green's function between two sensors can be reconstructed from the correlation of ambient seismic noise (Shapiro & Campillo 2004; Campillo 2006). This property has also been extensively used to image the Earth's interior at a global (Nishida *et al.* 2009), regional (Shapiro *et al.* 2005) and local scale (Brenguier *et al.* 2007; Masterlark *et al.* 2010). In this study, we use 10 yr of seismic noise records at Piton de la Fournaise (PdF) Volcano and follow the approach of Brenguier *et al.* (2008b) and Clarke *et al.* (2011) to measure continuous seismic velocity changes from ambient noise. We focus in particular on the 2007 March–April episode, during which we observe a large reduction in seismic velocity that has been previously reported by Brenguier *et al.* (2008b) and Duputel *et al.* (2009). The comparison between

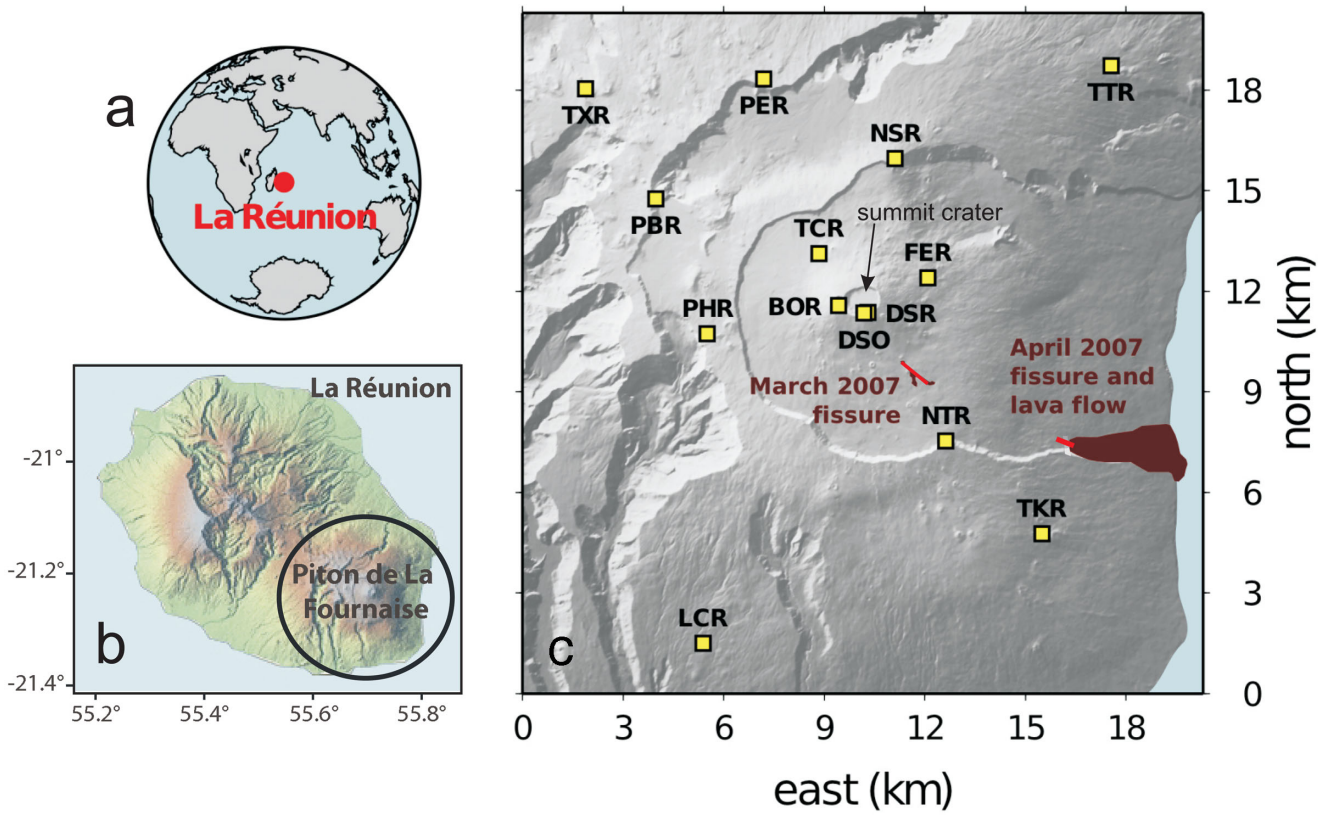

Figure 1. Maps showing the location of (a) La Réunion Island, (b) PdF volcano and (c) the short-period seismic stations used in this study (yellow squares). The 2007 March 30 and April 2 eruptive fissures (in red) and lava flows (in brown) are also plotted (from Staudacher *et al.* 2009).

these continuous seismic velocity changes and surface deformation observed using interferometric synthetic aperture radar (InSAR) and global positioning system (GPS) measurements allows us to infer that the 2007 March 30 dyke injection and the following lateral magma migration preceding the 2007 April eruption probably triggered and drove a widespread flank movement.

2 THE 2007 APRIL ERUPTION OF PdF

PdF (Fig. 1) is the youngest of three volcanoes that have contributed to the construction of La Réunion Island over its five million yr history and is likely the most recent manifestation of the mantle plume responsible for the formation of India's Deccan traps (Duncan *et al.* 1989). The 2632-m high basaltic shield volcano became active around 0.5 Ma (Gillot & Nativel 1989) and has undergone at least 12 significant mass wasting events during its relatively short history (Oehler *et al.* 2008; Le Friant *et al.* 2011), mostly on its unbuttressed eastern and southern flanks. For example, the eastern flank depression of the volcano is the scar of one of the most recent of these landslides, which took place around 5000 yr ago (Oehler *et al.* 2008).

Recently, PdF has been extremely active, erupting 34 times between 1998 and 2011 (Peltier *et al.* 2009a; Roult *et al.* 2012). These eruptions are generally small effusive events that last a few days to a few months. On 2007 April 2, however, a much larger eruption occurred on the volcano's southeastern flank, ejecting a volume of over 240 $\times$ 10^6 m^3 of lava—10 times more than the typical eruptive volume during the preceding decade (Bachèlery *et al.* 2010). The 2007 April 2 event was preceded by a smaller eruption, which lasted only a few hours, on 2007 March 30. A few days later (2007 April 5), the summit crater collapsed by 340 m (Staudacher *et al.* 2009). This 2007 April volcanic episode led to a remarkable change of behaviour of the volcano (Peltier *et al.* 2010).

3 LONG-TERM SEISMIC VELOCITY CHANGE MEASUREMENTS OVER 10 YR AND THE ANOMALOUS 2007 MARCH–APRIL ERUPTIONS

We use 10 yr of seismic noise recorded by the PdF Volcano Observatory short-period seismic network (Fig. 1c) and follow the approach of Brenguier *et al.* (2008b) to measure continuous seismic velocity changes associated with the 2007 March–April episode. We use reference cross-correlation functions that are obtained by cross-correlating all available seismic noise records at different seismic stations between 2000 and 2010 and compare them to current cross-correlation functions that are obtained by cross-correlating a given number of days of seismic noise at a time. Before correlation, ambient noise records are whitened in the frequency range 0.1–1 Hz, and one-bit normalization is applied. We take into account only stations for which continuous waveforms are available over the full 10-yr period. This is to ensure that the observed seismic velocity fluctuations are not due to changes in the network configuration. As in Clarke *et al.* (2011) for each current function, we obtain a series of time-shift (δt) measurements by comparison with reference correlation functions using the Moving-Window Cross-Spectral technique (Poupinet *et al.* 1984; Ratdomopurbo & Poupinet 1995). Here, the cross-correlations are divided into windows with central correlation time t. Within each window, δt is measured from the phase of the cross-spectrum of the two cross-correlation functions. If we assume

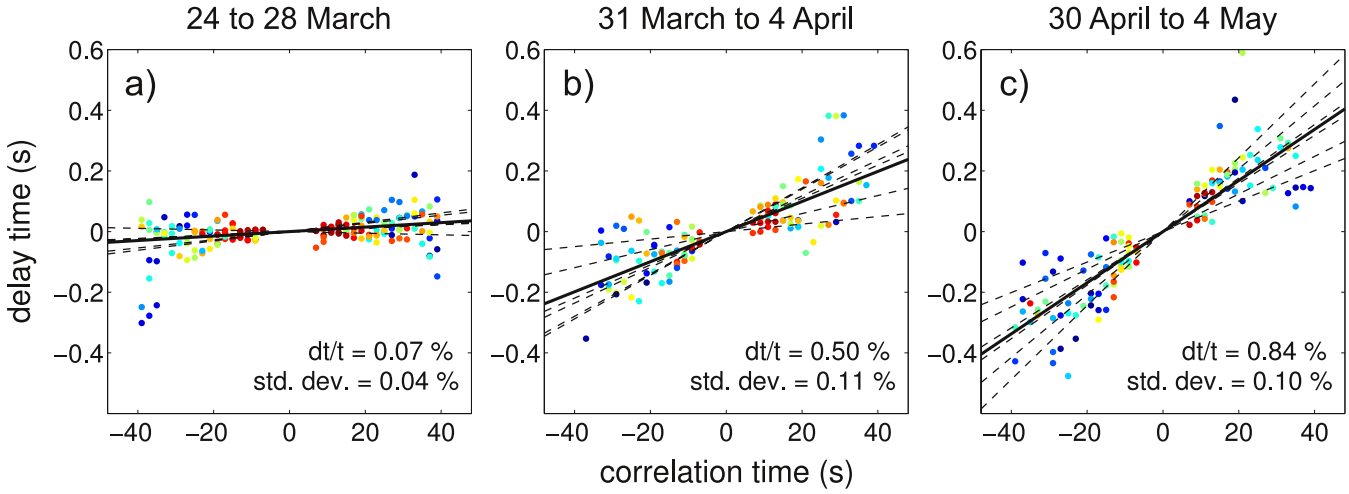

Figure 2. Delay times measured at stations BOR, DSR, FLR and TCR (a) before, (b) during and (c) after the 2007 March 30 and April 2 eruptions. Colours indicate the mean coherence between current cross-correlations (5 d) and reference cross-correlations (2007 January 1 to 2007 March 29) and range between 0.8 (blue) and 1.0 (red). Dashed lines show $\delta t/t$ for each station pair, while the solid line shows their average. Intercept times are removed prior to plotting.

that the current cross-correlation is perturbed by a homogeneous seismic velocity change, then $\delta v/v = -\delta t/t$, which we measure using a linear regression of δt and t over all windows. This method is illustrated in Fig. 2, which shows delay times from three distinct periods: before (Fig. 2a), during (Fig. 2b) and after (Fig. 2c) the eruptions of 2007 March and April. In this example, we use 5 d of ambient noise to compute current cross-correlation functions for summit stations BOR, DSR, FLR and TCR. For each pair of stations, $\delta t/t$ is estimated (dashed lines) along with an intercept time. To obtain a spatially averaged value of $\delta t/t$, we take the mean measurement (solid line) for all station pairs. In this example, $\delta t/t$ is less than 0.1 per cent before the 2007 March 30 eruption, but increases to 0.5 per cent by the time of the collapse of the summit crater on 2007 April 5. This trend is interrupted by a period of poorly constrained measurements during the crater collapse and then resumes as the eruption continues. After this period, the delay times are systematically perturbed and $\delta t/t$ is increased to around 0.8 per cent.

Fig. 3 shows the relative seismic velocity reduction over 10 yr averaged over all station pairs available across the PdF edifice. Here, we use 30 d of ambient noise to compute current cross-correlation functions. There is a strong decrease in seismic velocity (−0.6 per cent) that occurred in 2007 March–April. In contrast, typical pre-eruptive seismic velocity reductions observed at PdF are of the order of 0.1 per cent (Brenguier *et al.* 2008b). Those changes are interpreted as being induced by the opening of cracks associated with the summit inflation during periods of unrest and dyke intrusion. In the following, we will focus on the 2007 March–April time period to better understand the origin of the velocity reduction of 0.6 per cent.

4 DETECTION OF WIDESPREAD FLANK MOVEMENT BY InSAR

Since mid-2003, regular InSAR monitoring of the activity of PdF has been carried out by the Observatoire de Physique du Globe de Clermont-Ferrand (Froger *et al.* 2004). The 2007 April eruption is the first example of an eruptive crisis imaged simultaneously by the C-band advanced synthetic aperture radar (ASAR) on board the

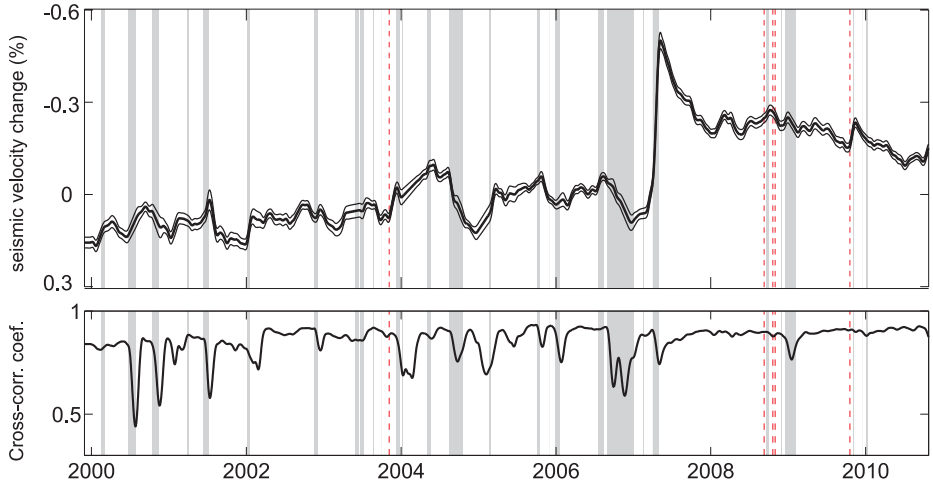

Figure 3. Seismic velocity variations for the time period between 2000 and 2010 (velocity decrease is upwards). Measurements are from 30-d cross-correlations and are smoothed using a 15-d sliding mean. Average velocity variations (thick black line) and standard deviations (thin black lines) are shown (top plot). We also show the averaged correlation coefficient between current and reference cross-correlation functions measured for all available stations (bottom plot). Vertical grey bars mark periods of eruptive activity and red dashed lines show the timing of intrusions.

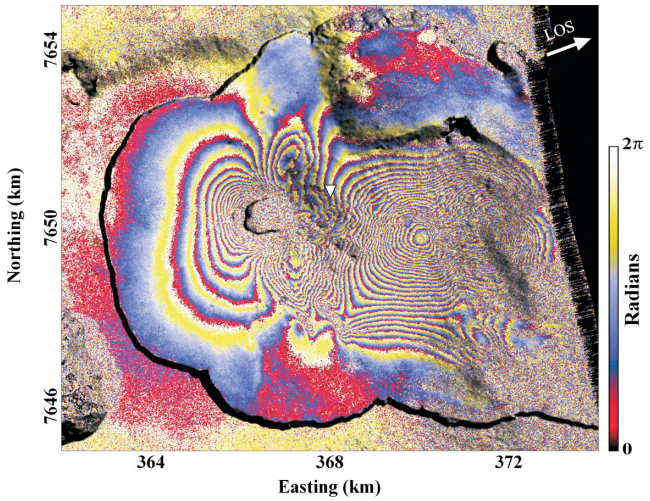

Figure 4. ASAR ascending interferogram spanning 35 d from 2007 March 26 to April 30. The phases have been draped on the shaded relief of PdF. A complete cycle of phase (red–blue–yellow) represents an increase in range of 2.8 cm between the ground surface and the satellite. The white arrow indicates the Line of Sight (LOS). The inverted white triangle shows the position of GPS station FERg.

European satellite ENVISAT and by the Phased Array L-band Synthetic Aperture Radar (PALSAR) on board the Japanese satellite ALOS. Three ASAR and two PALSAR interferograms spanning the 2007 March–April period were produced using the two-pass method described by Massonnet & Feigl (1998). The topographic contribution to the interferograms was removed using a 25-m Digital Elevation Model made in 1997 by the French Geographic Institute. The interferograms were unwrapped using the Snaphu unwrapper (Chen & Zebker 2000). As an example, the ASAR ascending interferogram spanning 35 d from 2007 March 26 to 2007 April 30 is shown in Fig. 4. The horizontal and vertical components of co-eruptive displacements (EW and vertical) were inverted from the unwrapped phases using the approach of Wright *et al.* (2004). On the resulting displacement maps, three main signals are visible (Fig. 5):

First, the entire western part of the central cone of PdF is affected both by eastward and downward displacement, indicating subsidence with a maximum of about 50 cm at the northwestern rim of the summit crater. This subsidence is interpreted as a joint effect of (1) the result of the fast draining of the shallow magma reservoir during the 2007 April eruption, (2) the elastic response of the edifice associated with the crater collapse itself and (3) the result of the large and rapid depressurization of a hydrothermal system within the central cone when the summit crater collapsed on 2007 April 5 (Michon *et al.* 2009; Peltier *et al.* 2009b; Staudacher *et al.* 2009).

Secondly, the displacement maps reveal a large inflation axis that extends N-S for about 4 km along the eastern part of the central cone (Fig. 5b). The horizontal component indicates a total opening of about 20 cm in the EW direction in the northern part of the axis and up to 45 cm in the EW direction in the southern part of the axis (Fig. 5a). The vertical component exhibits a maximum uplift of about 25 cm on the southeastern flank of the central cone. At its southern end, the N-S axis divides in two parallel branches oriented at azimuths of 150°. The easternmost branch coincides with the location of the 2007 March 30 eruptive fissure, suggesting that the whole N-S uplift was caused by the 2007 March 30 intrusion and eruption.

Finally, the eastern flank of the volcano is marked by a large displacement pattern. On the horizontal component map, the pattern covers a roughly triangular area of about 4.5 by 4 km, indicating eastward displacement with a maximum of 1.4 m. The vertical component map shows a more complicated pattern, with subsidence of the eastern flank of up to 33 cm, intersected in its central part by uplift reaching 37 cm.

These observations suggest the superposition of a large-wavelength downslope sliding of the entire eastern flank, except its southern part, and a shorter wavelength uplift of its central part. There is no clear evidence for large elastic deformation induced by the 2007 April 2 dyke intrusion. The associated deformation might be concealed by the flank motion. Thus, the observations made with InSAR during the 2007 April eruption provide direct evidence of a large seaward displacement affecting the eastern flank of PdF. An uncertainty arises, however, from the fact that the co-eruptive

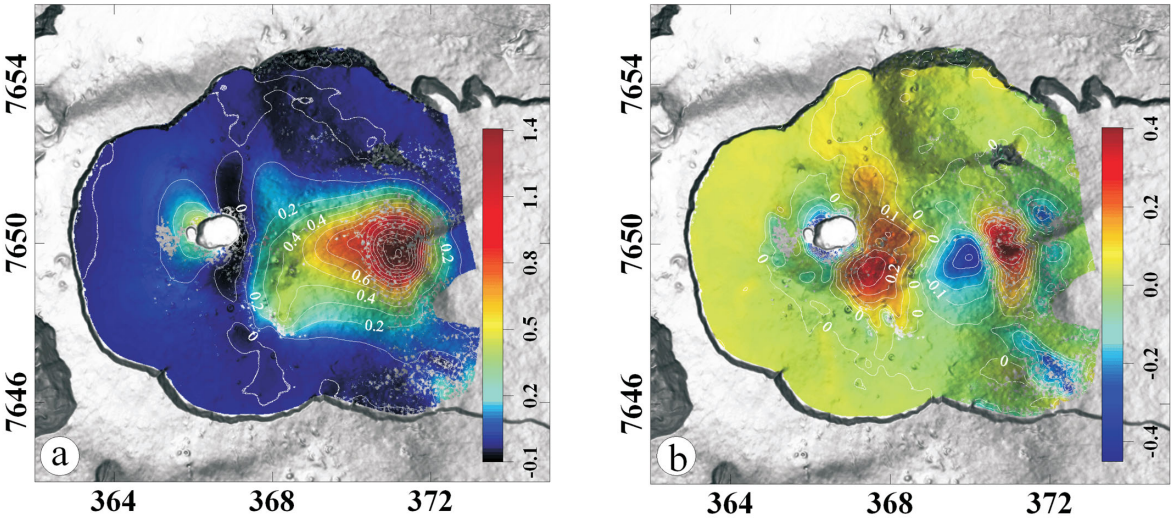

Figure 5. InSAR-derived co-eruptive (2007 March–April) displacements (metres) draped on the shaded relief of PdF. (a) E–W component, contour interval is 0.1 m. (b) Vertical component, contour interval is 0.1 m. The displacements were inverted using the approach from Wright *et al.* (2004) using two ascending PALSAR interferograms, two ascending ASAR interferograms and one descending ASAR interferogram spanning the 2007 March 4–April 19, the 2007 February 20–May 23, the 2007 March 20–April 24, the 2007 March 26–April 30 and the 2007 March 18–April 22 periods, respectively.

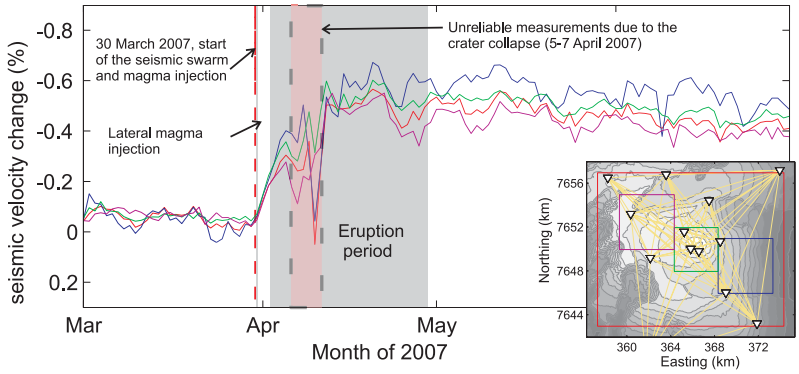

Figure 6. Seismic velocity variations around the time of the 2007 April eruption (velocity decrease is upwards). Measurements are from 5-d cross-correlations. Each velocity change measurement is plotted at the end of the 5-d averaging window. Blue, green, red and purple curves represent the averaged seismic velocity variations over the eastern flank, the central cone, the whole network and the western area, respectively. Inset shows the areas used for seismic velocity variation spatial averaging.

InSAR data integrate all the events that occurred during the March–April period and, therefore, do not allow us to determine the time history of the displacements measured in the eastern flank, nor to understand their timing with respect to the eruptions on 2007 March 30 and April 2 and the collapse on 2007 April 5. In the following, we will use continuous measurements of temporal changes in seismic velocities and surface deformation to better constrain the timing of this movement.

5 OBSERVATIONS OF SEISMIC VELOCITY CHANGES DURING THE 2007 MARCH–APRIL EPISODE

To focus on the 2007 March–April episode, we plot the velocity variations obtained using 5-d current correlation functions for the period between 2007 March and June using the stations shown on Fig. 6. By using a shorter current window (5 d), we improve the temporal resolution of our measurements at the expense of their quality (Larose *et al.* 2008). More stations are available during this limited time period than for the entire 10 yr, allowing us to improve the accuracy of the measured velocity variations. We thus compensate for the loss in seismic velocity measurement quality by adding more stations during the 2007 time period. By adding more data and applying a refined processing as described in Clarke *et al.* (2011), we are able to obtain more reliable measurements than in Brenguier *et al.* (2008b) for this time period.

Each velocity change measurement is plotted at the end of the 5-d averaging window. We regionalize the observed relative velocity variations over the surface of PdF. For each station pair, we assign $\delta v/v$ to a set of 1 km^2 cells for which $a + b \leq d + 2$ km, where a and b are the distances between the cell centre and each station, and d is the interstation separation. We then average the associated values of $\delta v/v$ within each cell (Brenguier *et al.* 2008b). Finally, we compute the velocity variations averaged over different areas of the volcanic edifice. Fig. 6 shows that the amplitude of velocity reduction is highest within the eastern flank area (blue curve). Moreover, we observe that the velocity reduction starts on 2007 March 30 and reached its maximum level of -0.6 per cent on April 15, 16 d after the first eruption. The strong fluctuations in seismic velocities during the crater collapse are still not explained and may be partly due to unreliable measurements. Also, because of a loss in coherence of the cross-correlation functions during the 2007 April eruption and to a low seismic station coverage of the eastern flank of the volcano, the error of seismic velocity measurements for the eastern par of the volcano (blue curve) is of the order of 0.2 per cent which is the order of difference between seismic velocity changes for the eastern and western part of the volcano. However, there is a constant difference during the entire pre-eruptive and eruptive period of 2007 April between the eastern and western velocity changes which we think is a good marker for an overall higher velocity decrease of the eastern flank of the volcano.

Previous studies have reported that the magma injection from the central area towards the eastern flank and 2007 April 2 eruptive fissure started at the time of the 2007 March 30 eruption (Peltier *et al.* 2009b; Massin *et al.* 2011). The strong velocity decrease starting on 2007 March 30 thus initiates at the same time as the dyke injection feeding the 2007 March 30 eruption and as the lateral magma injection towards the 2007 April 2 eruptive fissure. The cumulative amount of velocity reduction prior to the 2007 April 2 eruption is -0.2 per cent. Seismic velocities continued to decrease until 2007 April 15 and reached a level of -0.6 per cent. This may be due to the slow movement of the eastern flank, but might also be partly due to the collapse of the summit crater on 2007 April 5–7, which strongly damaged the summit edifice area.

6 OBSERVATIONS OF GROUND DISPLACEMENTS (GPS) DURING THE 2007 MARCH–APRIL EPISODE

Since 2004, ground deformation of the PdF edifice has been monitored by a GPS network run by the PdF Volcano Observatory. The main observations of GPS displacements associated with the 2007 April eruption and crater collapse have been described in Staudacher *et al.* (2009) and Peltier *et al.* (2009b). Here, we focus on the observation of markers of the studied movement of the eastern flank. Figs 7 and 8 show the surface displacements measured using permanent GPS receivers operating on PdF for the time period preceding the 2007 March 30 eruption and following the 2007 April 5–7 crater collapse. Relative baseline changes for the summit area over a few years (including 2007) are shown in Fig. 7(a) and for the 2007 March–April episode in Fig. 7(b). The baseline change measurements are an indicator of summit deformation. Steps in the baseline changes curve seen in Fig. 7(a) (e.g. 2007 February) correspond to dyke injections. These observations show that the summit experienced a 6-week inflation prior to the 2007 March–April eruption, then a strong deflation that began at the time of the 2007 April 5 crater collapse. It can be clearly seen on Figs 7(a) and (b) that no strong summit deformation occurs prior to the 2007 April 2

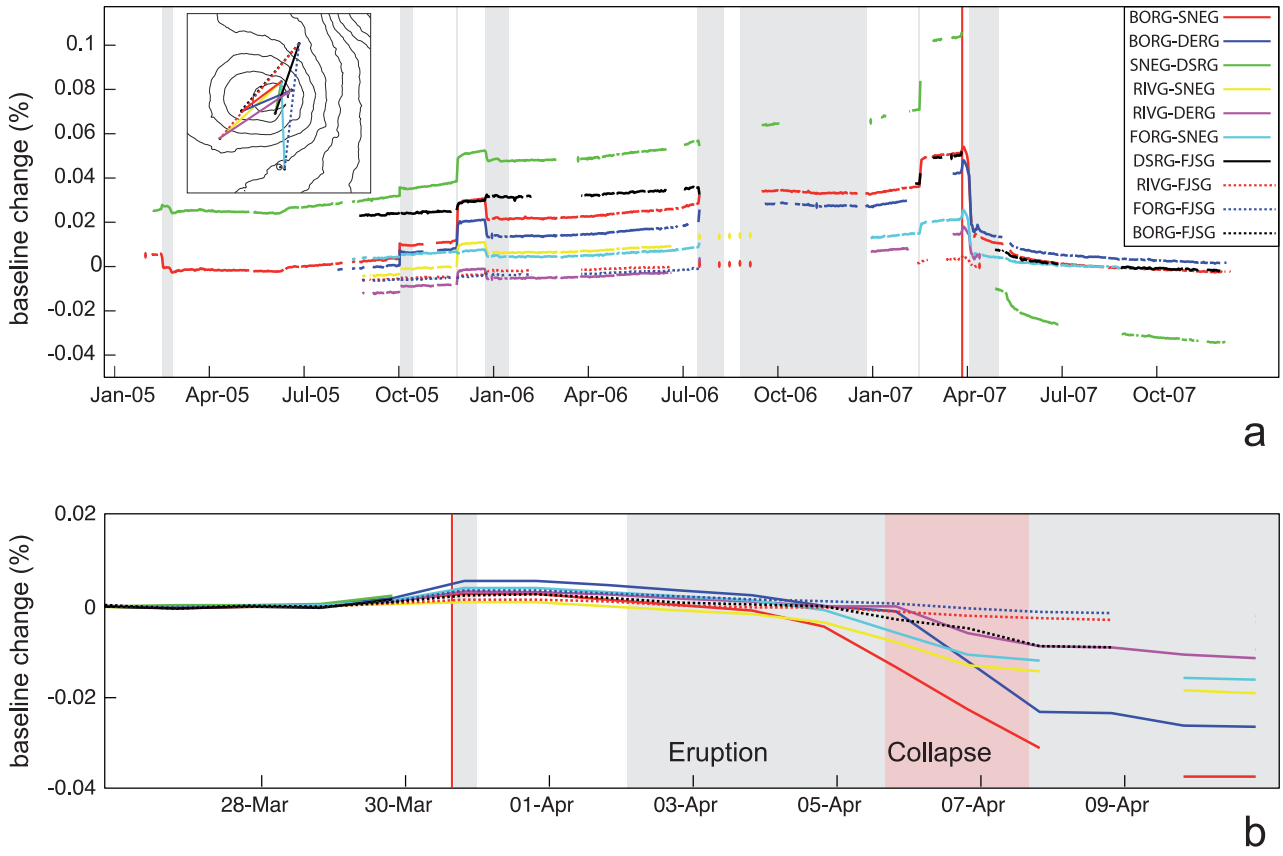

Figure 7. Daily GPS baseline changes across the central part of PdF. (a) Relative change in per cent for baselines crossing the summit crater as shown on the inset figure. Grey boxes show the time of eruptions. The red bar corresponds to the 2007 March 30 magma injection. (b) Relative baseline change in per cent during the 2007 March–April volcanic episode.

eruption. There is therefore no strong summit deformation that could explain the strong reduction of seismic velocity starting on 2007 March 30.

The white vectors on Fig. 8(a) show the displacements induced by the dyke injection preceding the 2007 March 30 eruption. All GPS stations except FERg show a displacement trend that can be explained by the elastic response of the edifice to the 2007 March 30 intrusion and eruption. By contrast, station FERg, located on the upper eastern flank, clearly shows a change in the displacement trend following the 2007 March 30 dyke injection towards the southeast that cannot be explained by the elastic response to the intrusion. Fig. 8(b) also shows that this change in the displacement trend started at the time of the 2007 March 30 dyke injection and that most of this displacement occurred before the 2007 April 2 eruption. This displacement towards the southeast reaches 0.15 m on 2007 April 2, which is consistent with InSAR deformation shown on Fig. 5. We thus interpret this observed southeastern displacement of the upper eastern flank as being associated with the widespread flank movement detected by InSAR.

7 DISCUSSION AND CONCLUSIONS

Seismic velocity reduction measurements show that a strong decrease in seismic velocity affected PdF during the volcanic episode of 2007 March–April. InSAR deformation maps show that widespread deformation of PdF's eastern flank occurred during the same time period. Refined measurements also show that the observed strong reduction in seismic velocity is greatest on the PdF eastern flank and that it started on 2007 March 30, a few days before the 2007 April 2 eruption. Finally, GPS measurements show that the uppermost eastern flank started moving to the southeast at the time of the 2007 March 30 dyke injection and continued moving until the beginning of the 2007 April 2 eruption.

We therefore propose that the sudden southeast displacement of the uppermost eastern flank measured using GPS is a marker for the beginning of the widespread flank movement imaged using InSAR. We also propose that the unusually high seismic velocity reduction starting on 2007 March 30 is induced by this widespread flank movement. We believe that the widespread movement of the eastern flank was triggered at the beginning of the lateral magma migration preceding the 2007 April eruption.

From the InSAR maps, we can infer that the eastern flank experienced a widespread deformation of the order of 10^{-4} strain (volume increase). For such a large deformation, strong seismic velocity decreases in rocks have been previously observed (e.g. Johnson & Rasolofosaon 1996). Such a behaviour is referred as a non-linear elastic regime when strain affects the rock elastic modulus. Moreover, according to previous studies (Brenguier *et al.* 2007) and considering the assumption that at frequencies between 0.1 and 1 Hz, the reconstructed correlation function coda waves are mainly surface waves, we argue that the observed seismic velocity changes are a depth average of velocity changes occurring from the surface to about 3 km depth. As a consequence, if the strong velocity drop is associated with a shallow flank movement (of a few hundreds of metres thickness), the actual velocity change in that perturbed layer should be around a few per cent, which is in agreement with Birch (1966) and Johnson & Rasolofosaon (1996).

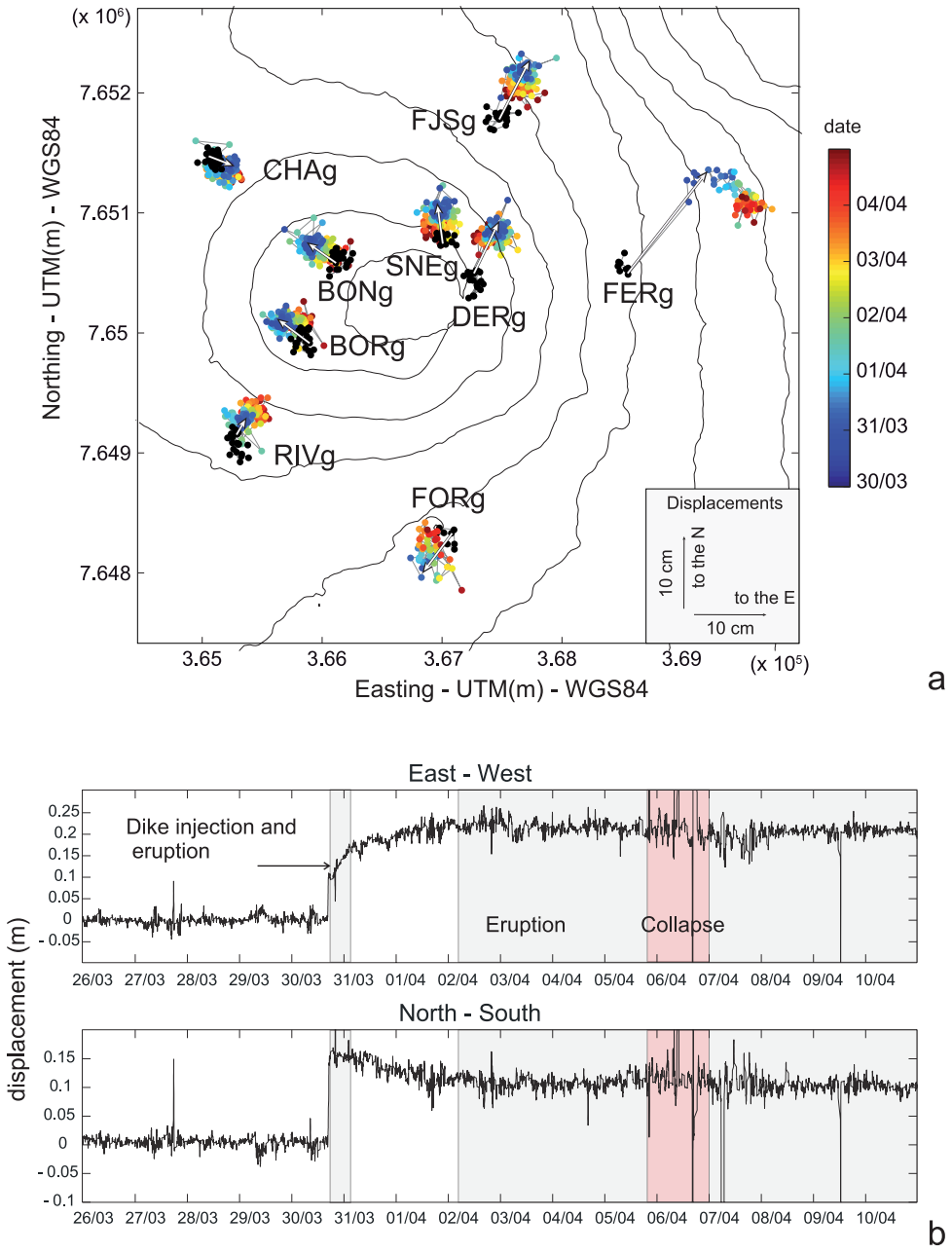

Figure 8. GPS displacements during the March–April volcanic episode (one point every 1 hr). (a) Map of GPS displacements between 2007 March 30 and April 5. The white vectors illustrate the cumulative displacements induced by the dyke injection preceding the 2007 March 30 eruption. Black dots represent the GPS positions a few days before 2007 March 30. (b) East–west and north–south displacements at station FERg. These displacements increase eastwards and northwards, respectively.

Finally, we believe that the widespread movement of the eastern flank may partly control the lateral migration of magma over long distances, and the occurrence of the 2007 April 2 eruption. Such a feedback process has already been proposed by Owen *et al.* (2000) and Cervelli *et al.* (2002) at Kilauea and Walter *et al.* (2005) at Mount Etna. The release of stress induced by the flank movement could have favoured the withdrawal of the large volume of magma during the 2007 April 2 eruption. Moreover, the collapse of the summit crater would result from this large withdrawal of magma (Staudacher *et al.* 2009).

This study presents a new observation of continuous seismic velocity change derived from ambient noise measurements. Overall, it emphasizes the potential of this new method, together with geodetic observations, to detect and monitor possible hazardous slope instabilities.

ACKNOWLEDGEMENTS

All seismic and GPS data used in this study were acquired by the Piton de la Fournaise Volcano Observatory, Institut de Physique du Globe de Paris (OVPF, IPGP). We are grateful to Valérie Ferrazzini and Andrea Di Muro for fruitful discussions. We acknowledge Michael Poland and an anonymous reviewer for valuable comments on the manuscript. ASAR and PALSAR data were provided by the European Space Agency (ESA) through the AO ENVISAT project 746 and the ALOS-ADEN project 3622. The interferograms were

processed using the DIAPASON software package (CNES/Altamira Information). This work has been supported by ANR (France) under contracts ANR-06-CEXC-005 (COHERSIS), ANR-08-RISK-011 (UNDERVOLC), by a FP7 European Research Council advanced grant 227507 (WHISPER), and by *Emergences2011* grant from the city of Paris. This is IPGP contribution number 3404.

REFERENCES

Alidibirov, M. & Dingwell, D.B., 1996. Magma fragmentation by rapid decompression, *Nature,* **380**(6570), 146–148.

Bachèlery, P. *et al.*, 2010. Huge lava flow into the sea and caldera collapse, April 2007, Piton de la Fournaise, in *IAVCEI Third Workshop on Collapse Calderas, La Réunion,* pp. 73–74.

Birch, F., 1966. Compressibility, Elastic constants, in *Handbook of Physical Constants,* Geol. Soc. Am. Press.

Brenguier, F., Shapiro, N., Campillo, M., Nercessian, A. & Ferrazzini, V., 2007. 3-D surface wave tomography of the Piton de la Fournaise volcano using seismic noise correlations, *Geophys. Res. Lett.,* **34**(2), L02305, doi:10.1029/2006GL028586.

Brenguier, F., Campillo, M., Hadziioannou, C., Shapiro, N.M., Nadeau, R.M. & Larose, E., 2008a. Postseismic relaxation along the San Andreas fault at Parkfield from continuous seismological observations, *Science,* **321**(5895), 1478–1481.

Brenguier, F., Shapiro, N., Campillo, M., Ferrazzini, V., Duputel, Z., Coutant, O. & Nercessian, A., 2008b. Towards forecasting volcanic eruptions using seismic noise, *Nature Geosci.,* **1**(2), 126–130.

Calvari, S., Tanner, L.H. & Groppelli, G., 1998. Debris-avalanche deposits of the Milo Lahar sequence and the opening of the Valle del Bove on Etna volcano (Italy), *J. Volc. Geotherm. Res.,* **87**(1–4), 193–209.

Campillo, M., 2006. Phase and correlation in random seismic fields and the reconstruction of the Green function, *Pure appl. Geophys.,* **163,** 475–502.

Cervelli, P., Segall, P., Amelung, F., Garbeil, H., Meertens, C., Owen, S., Miklius, A. & Lisowski, M., 2002. The 12 September 1999 Upper East Rift Zone dike intrusion at Kilauea Volcano, Hawaii, *J. geophys. Res.,* **107**(B7), 2150, doi:10.1029/2001JB000602.

Chen, C. & Zebker, H., 2000. Network approaches to two-dimensional phase unwrapping: intractability and two new algorithms, *J Opt. Soc. Am. A,* **17**(3), 401–414.

Clarke, D., Zaccarelli, L., Shapiro, N.M. & Brenguier, F., 2011. Assessment of resolution and accuracy of the Moving Window Cross Spectral technique for monitoring crustal temporal variations using ambient seismic noise, *Geophys. J. Int.,* **186**(2), 867–882.

De Vries, B.V.W. & Francis, P., 1997. Catastrophic collapse at stratovolcanoes induced by gradual volcano spreading, *Nature,* **387**(6631), 387–390.

Devoli, G., Cepeda, J. & Kerle, N., 2009. The 1998 Casita volcano flank failure revisited—new insights into geological setting and failure mechanisms, *Eng. Geol.,* **105**(1–2), 65–83.

Duncan, R.A., Backman, J. & Peterson, L., 1989. Reunion hotspot activity through tertiary time: initial results from the ocean drilling program, leg 115, *J. Volc. Geotherm. Res.,* **36**(1–3), 193–198.

Duputel, Z., Ferrazzini, V., Brenguier, F., Shapiro, N., Campillo, M. & Nercessian, A., 2009. Real time monitoring of relative velocity changes using ambient seismic noise at the Piton de la Fournaise volcano (La Reunion) from January 2006 to June 2007, *J. Volc. Geotherm. Res.,* **184**(1–2, Sp. Iss. SI), 164–173.

Famin, V. & Michon, L., 2010. Volcano destabilization by magma injections in a detachment, *Geology,* **38**(3), 219–222.

Francis, P.W., Gardeweg, M., Ramirez, C.F. & Rothery, D.A., 1985. Catastrophic debris avalanche deposit of Socompa volcano, northern Chile, *Geology,* **13**(9), 600–603.

Froger, J.-L., Fukushima, Y., Briole, P., Staudacher, T., Souriot, T. & Villeneuve, N., 2004. The deformation field of the August 2003 eruption at Piton de la Fournaise, Reunion Island, mapped by ASAR interferometry, *Geophys. Res. Lett.,* **31,** L14601, doi:10.1029/2004GL020479.

Gillot, P.Y. & Nativel, P., 1989. Eruptive history of the Piton de la Fournaise Volcano, Réunion Island, Indian Ocean, *J. Volc. Geotherm. Res.,* **36**(1–3), 53–65.

Johnson, P. & Rasolofosaon, P., 1996. Manifestation of nonlinear elasticity in rock: convincing evidence over large frequency and strain intervals from laboratory studies, *Nonlinear Process. Geophys.,* **3**(2), 77–88.

Labazuy, P., 1996. Recurrent landslides events on the submarine flank of Piton de la Fournaise volcano (Reunion Island), *J. Geol. Soc.,* **110,** 295–306.

Larose, E., Roux, P., Campillo, M. & Derode, A., 2008. Fluctuations of correlations and Green's function reconstruction: role of scattering, *J. appl. Phys.,* **103**(11), 114 907–114 916.

Le Friant, A., Lebas, E., Clément, V., Boudon, G., Deplus, C., de Voogd, B. & Bachèlery, P., 2011. A new model for the evolution of La Réunion volcanic complex from complete marine geophysical surveys, *Geophys. Res. Lett.,* **38,** L09312, doi:10.1029/2011GL047489.

Lipman, P.W. & Mullineaux, D., Eds. 1981. *The 1980 Eruptions of Mount St. Helens, Washington,* Vol. 1250 of US Geological Survey Professional Paper, United States Government Printing Office, Washington, DC.

Lipman, P.W., Normark, W.R., Moore, J.G., Wilson, J.B. & Gutmacher, C.E., 1988. The giant submarine Alika debris slide, Mauna Loa, Hawaii, *J. geophys. Res.,* **93**(B5), 4279–4299.

Massin, F., Ferrazzini, V., Bachèlery, P., Nercessian, A., Duputel, Z. & Staudacher, T., 2011. Structures and evolution of the plumbing system of Piton de la Fournaise volcano inferred from clustering of 2007 eruptive cycle seismicity, *J. Volc. Geotherm. Res.,* **202**(1–2), 96–106.

Massonnet, D. & Feigl, K., 1998. Radar interferometry and its application to changes in the Earth's surface, *Rev. Geophys.,* **36**(4), 441–500.

Masterlark, T., Haney, M., Dickinson, H., Fournier, T. & Searcy, C., 2010. Rheologic and structural controls on the deformation of Okmok volcano, Alaska: FEMs, InSAR, and ambient noise tomography, *J. geophys. Res.,* **115,** B02409, doi:10.1029/2009JB006324.

McGuire, W.J., 1996. Volcano instability: a review of contemporary themes, in *Volcano Instability on the Earth and Other Planets,* Geological Society Special Publication 110, pp. 1–23.

Michon, L., Villeneuve, N., Catry, T. & Merle, O., 2009. How summit calderas collapse on basaltic volcanoes: new insights from the April 2007 caldera collapse of Piton de la Fournaise volcano, *J. Volc. Geotherm. Res.,* **184**(1), 138–151.

Moore, J.G., Clague, D.A., Holcomb, R.T., Lipman, P.W., Normark, W.R. & Torresan, M.E., 1989. Prodigious submarine landslides on the Hawaiian ridge, *J. geophys. Res.,* **94**(B12), 17 465–17 484.

Mordret, A., Jolly, A.D., Duputel, Z. & Fournier, N., 2010. Monitoring of phreatic eruptions using Interferometry on Retrieved Cross-Correlation Function from ambient seismic noise: results from Mt. Ruapehu, New Zealand, *J. Volc. Geotherm. Res.,* **191**(1–2), 46–59.

Nishida, K., Montagner, J. & Kawakatsu, H., 2009. Global surface wave tomography using seismic hum, *Science,* **326**(5949), 112.

Oehler, J.F., Lénat, J.F. & Labazuy, P., 2008. Growth and collapse of the Reunion Island volcanoes, *Bull. Volcanol.,* **70**(6), 717–742.

Owen, S., Segall, P., Lisowski, M., Miklius, A., Murray, M., Bevis, M. & Foster, J., 2000. January 30, 1997 eruptive event on Kilauea volcano, Hawaii, as monitored by continuous GPS, *Geophys. Res. Lett.,* **27**(17), 2757–2760.

Pareschi, M.T., Boschi, E., Mazzarini, F. & Favalli, M., 2006. Large submarine landslides offshore Mt. Etna, *Geophys. Res. Lett.,* **33,** L13302, doi:10.1029/2006GL026064.

Peltier, A., Bachelery, P. & Staudacher, T., 2009a. Magma transport and storage at Piton de La Fournaise (La Réunion) between 1972 and 2007: a review of geophysical and geochemical data, *J. Volc. Geotherm. Res.,* **184**(1–2, Sp. Iss. SI), 93–108.

Peltier, A., Staudacher, T., Bachèlery, P. & Cayol, V., 2009b. Formation of the April 2007 caldera collapse at Piton de La Fournaise volcano: insights from GPS data, *J. Volc. Geotherm. Res.,* **184**(1–2, Sp. Iss. SI), 152–163.

Peltier, A., Staudacher, T. & Bachèlery, P., 2010. New behaviour of the Piton de la Fournaise volcano feeding system (La Réunion Island) deduced from GPS data: influence of the 2007 Dolomieu caldera collapse, *J. Volc. Geotherm. Res.,* **192**(1), 48–56.

Poupinet, G., Ellsworth, W. & Frechet, J., 1984. Monitoring velocity variations in the crust using earthquake doublets: an application to the Calaveras faults, California, *J. geophys. Res.,* **89,** 5719–5731.

Ratdomopurbo, A. & Poupinet, G., 1995. Monitoring a temporal change of seismic velocity in a volcano: application to the 1992 eruption of Mt. Merapi (Indonesia), *Geophys. Res. Lett.,* **22**(7), 775–778.

Roult, G., Peltier, A., Taisne, B., Staudacher, T., Ferrazzini, V., Di Muro, A. & the OVPF team, 2012. A new comprehensive classification of the Piton de la Fournaise activity spanning the 1985–2010 period. Search and analysis of short-term precursors from a broad-band seismological station, *J. Volc. Geotherm. Res.,* **241–242,** 78–104.

Sens-Schönfelder, C. & Wegler, U., 2006. Passive image interferometry and seasonal variations of seismic velocities at Merapi Volcano, Indonesia, *Geophys. Res. Lett.,* **33,** L21302, doi:10.1029/2006GL027797.

Shapiro, N., Campillo, M., Stehly, L. & Ritzwoller, M., 2005. High-resolution surface-wave tomography from ambient seismic noise, *Science,* **307**(5715), 1615–1618.

Shapiro, N.M. & Campillo, M., 2004. Emergence of broadband Rayleigh waves from correlations of the ambient seismic noise, *Geophys. Res. Lett.,* **31,** L07614, doi:10.1029/2004GL019491.

Siebert, L., 1992. Volcano hazards—threats from debris avalanches, *Nature,* **356**(6371), 658–659.

Staudacher, T., Ferrazzini, V., Peltier, A., Kowalski, P., Boissier, P., Catherine, P., Lauret, F. & Massin, F., 2009. The April 2007 eruption and the Dolomieu crater collapse, two major events at Piton de la Fournaise (La Réunion Island, Indian Ocean), *J. Volc. Geotherm. Res.,* **184**(1–2), 126–137.

Walter, T., Acocella, V., Neri, M. & Amelung, F., 2005. Feedback processes between magmatic events and flank movement at Mount Etna (Italy) during the 2002–2003 eruption, *J. geophys. Res.,* **110,** B10205, doi:10.1029/2005JB003688.

Ward, S.N. & Day, S., 2003. Ritter island volcano, lateral collapse and the tsunami of 1888, *Geophys. J. Int.,* **154**(3), 891–902.

Watts, A.B. & Masson, D.G., 1995. A giant landslide on the north flank of Tenerife, Canary Islands, *J. geophys. Res.,* **100**(B12), 24 487–24 498.

Wegler, U. & Sens-Schönfelder, C., 2007. Fault zone monitoring with passive image interferometry, *Geophys. J. Int.,* **168**(3), 1029–1033.

Wright, T., Parsons, B. & Lu, Z., 2004. Toward mapping surface deformation in three dimensions using InSAR, *Geophys. Res. Lett.,* **31**(1), L01607, doi:10.1029/2003GL018827.